Structure of the complex between triosephosphate isomerase and N-hydroxy-4-phosphono-butanamide: Binding at the active site despite an "open" flexible loop

ARTICLE *in* PROTEIN SCIENCE · DECEMBER 1992

Impact Factor: 2.85 · DOI: 10.1002/pro.5560011205 · Source: PubMed

7 AUTHORS, INCLUDING:

Christophe LMJ Verlinde
University of Washington Seattle
155 PUBLICATIONS **4,676** CITATIONS
SEE PROFILE

Tjaard Pijning
University of Groningen
48 PUBLICATIONS **817** CITATIONS
SEE PROFILE

Kor H. Kalk
University of Groningen
151 PUBLICATIONS **9,849** CITATIONS
SEE PROFILE

Fred R. Opperdoes
Université catholique de Louvain
240 PUBLICATIONS **11,044** CITATIONS
SEE PROFILE

Protein Science (1992), *1*, 1578–1584. Cambridge University Press. Printed in the USA.

Structure of the complex between trypanosomal triosephosphate isomerase and *N*-hydroxy-4-phosphono-butanamide: Binding at the active site despite an "open" flexible loop conformation

CHRISTOPHE L.M.J. VERLINDE,[1,4] CORNELIS J. WITMANS,[2] TJAARD PIJNING,[1] KOR H. KALK,[1] WIM G.J. HOL,[1,4] MIA CALLENS,[3] AND FRED R. OPPERDOES[3]

[1] BIOSON Research Institute, University of Groningen, The Netherlands
[2] University Centre for Pharmacy, University of Groningen, The Netherlands
[3] Institute for Cellular and Molecular Pathology, Research Unit for Tropical Diseases, Brussels, Belgium

(RECEIVED May 21, 1992; REVISED MANUSCRIPT RECEIVED August 4, 1992)

Abstract

The structure of triosephosphate isomerase from *Trypanosoma brucei* complexed with the competitive inhibitor *N*-hydroxy-4-phosphono-butanamide was determined by X-ray crystallography to a resolution of 2.84 Å. Full occupancy binding of the inhibitor is observed only at one of the active sites of the homodimeric enzyme where the flexible loop is locked in a completely open conformation by crystal contacts. There is evidence that the inhibitor also binds to the second active site of the enzyme, but with low occupancy. The hydroxamyl group of the inhibitor forms hydrogen bonds to the side chains of Asn 11, Lys 13, and His 95, whereas each of its three methylene units is involved in nonpolar interactions with the side chain of the flexible loop residue Ile 172. Interactions between the hydroxamyl and the catalytic base Glu 167 are absent. The binding of this phosphonate inhibitor exhibits three unusual features: (1) the flexible loop is open, in contrast with the binding mode observed in eight other complexes between triosephosphate isomerase and various phosphate and phosphonate compounds; (2) compared with these complexes the present structure reveals a 1.5-Å shift of the anion-binding site; (3) this is the first phosphonate inhibitor that is not forced by the enzyme into an eclipsed conformation about the P-CH_2 bond. The results are discussed with respect to an ongoing drug design project aimed at the selective inhibition of glycolytic enzymes of *T. brucei*.

Keywords: *N*-hydroxy-4-phosphono-butanamide; triosephosphate isomerase

Triosephosphate isomerase (TIM, EC 5.3.1.1) from *Trypanosoma brucei*, like eight other glycolytic enzymes sequestered in the glycosome of the pathogen of African sleeping sickness, is an attractive target for rational drug design (Hol, 1986; Opperdoes et al., 1990), because the bloodstream form of the parasite derives all of its energy from glycolysis (Fairlamb et al., 1985). The enzyme catalyzes the interconversion of dihydroxyacetonephosphate and D-glyceraldehyde-3-phosphate (Fig. 1a). The structure of trypanosomal TIM in 2.4 M ammonium sulfate has been determined by X-ray crystallographic methods (Wierenga et al., 1991b) together with the structures of the complexes with the competitive inhibitors glycerol 3-phosphate, 3-phosphoglycerate, 3-phosphonopropionate (Noble et al., 1991b), phosphate (Verlinde et al., 1991a), 2-phosphoglycerate (Noble et al., 1991a), and 2-(*N*-formyl-*N*-hydroxamino)ethylphosphonic acid (Witmans et al., unpubl.).

From these studies, the usefulness of the phosphate or phosphonate moiety as a molecular anchor for further inhibitor design has been established. Furthermore, residues Ala 100–Tyr 101 of the glycosomal enzyme (Swinkels et al., 1986), the loci of which are occupied by His-Val in

Reprint requests to: C.L.M.J. Verlinde, Department of Biological Structure, Health Sciences Building SM-20, School of Medicine, University of Washington, Seattle, Washington 98195.
[4] Present address: Department of Biological Structure, School of Medicine, University of Washington, Seattle, Washington 98195.

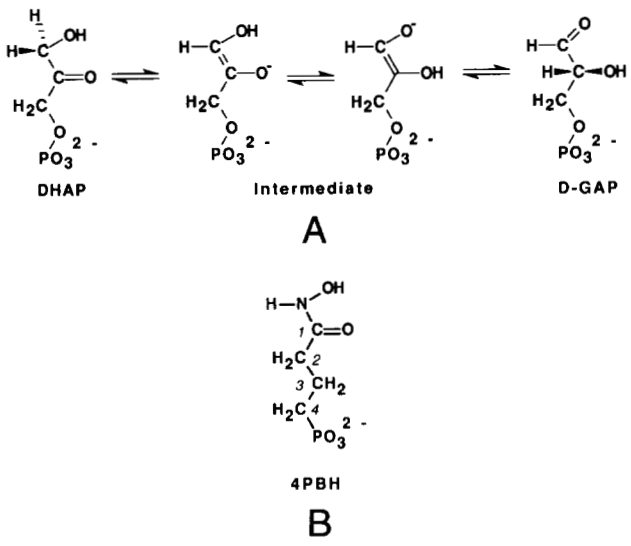

Fig. 1. A: The reaction catalyzed by TIM. A catalytic base, the carboxylate of Glu 167 (numbering according to the trypanosomal TIM sequence), abstracts the pro-*R* proton on C-1 of dihydroxyacetonephosphate (DHAP) yielding an enediolate intermediate, which then further collapses to D-glyceraldehyde-3-phosphate (D-GAP). The reaction is assisted by the neutral imidazole of His 95 (Knowles, 1991). **B:** Atomic numbering scheme of the active site inhibitor 4PBH.

human TIM (Maquat et al., 1985), were identified as a promising target for conferring selectivity for inhibitors (Verlinde et al., 1991b). However, the crystallographically studied inhibitors offer limited opportunities for modification in the direction of the species-specific sequence loci. Indeed, the flexible loop of the enzyme (residues 168–180; animated in Kinemage 2), essential for binding the enzymatic reaction intermediate in a conformation that disfavors the phosphate elimination side reaction (Pompliano et al., 1990), fully closes around all of these inhibitors. As a result, the only ligand atoms exposed to solvent are the phosphorus atom and the terminal oxygens attached to it (Noble et al., 1991b). It should be mentioned that in the crystal, the studied inhibitors bind only to the active site of subunit 2 of the homodimeric enzyme. Binding to subunit 1 has not been observed, possibly because binding to the oxyanion site is electrostatically hindered by the nearby presence of the carboxylate of Glu 323 of a symmetry-related protein molecule. Moreover, contacts with this neighboring molecule lock the flexible loop of subunit 1 in an open conformation (Wierenga et al., 1991a). In order to distinguish between residues from different subunits, residues from subunit 1 are numbered 2–250 and those of subunit 2 range from 302 to 550.

Inhibitors that have more than just the phosphate moiety exposed to the solvent would constitute more promising lead compounds for further selective inhibitor design. Therefore, we have tried to design phosphate/phosphonate compounds that would be too bulky to fit into the active site cleft of TIM in the hope that such compounds would be reoriented toward the outside of the protein or have their phosphate/phosphonate moiety substantially shifted. In both cases additional atoms might become available for proper modifications in the direction of residues Ala 400–Tyr 401.

Eventually, one of the designed compounds, *N*-hydroxy-4-phosphono-butanamide (hereafter abbreviated as 4PBH), was synthesized (Witmans et al., unpubl.) (Fig. 1b). This molecule possesses a hydroxamic acid, a function introduced by Collins (1974) as a mimetic of the enediolate reaction intermediate, but is conceptually one methylene unit longer than any chemical species present along the enzymatic reaction coordinate. Remarkably, it has proved to be a better inhibitor than any of the ligands we had studied crystallographically before. The K_i is 0.33 mM and 4PBH inhibits trypanosomal TIM in a competitive way with respect to D-glyceraldehyde-3-phosphate (M. Callens & F.R. Opperdoes, unpubl.). Described here is the surprising structure of the complex between trypanosomal TIM and 4PBH (Kinemage 1).

Results

4PBH binding by subunit 1

The present crystal structure provides a clear view of the stereochemistry of the 4PBH binding by the active site of subunit 1 of trypanosomal TIM, as can be judged from the fit of the ligand into omit density (Fig. 2). A more quantitative proof of the presence of the inhibitor is given by the signal of the individual atoms in the omit map (Table 1): the phosphonate and hydroxamyl moieties are well defined; only the central atom of the aliphatic chain, C3, has weak density. Furthermore, the individual atomic *B*-factors of 4PBH are quite acceptable (Table 1). They can be compared with an overall mean *B* for all atoms of the protein molecule of 20 Å^2. A further assessment of the reliability of the inhibitor model is the evaluation of the dihedral angles. The conformation of 4PBH is staggered about P-C4, antiperiplanar about C4-C3, antiperi-

Table 1. *Atomic B-factors (Å^2) of 4PBH after refinement together with the electron-density levels (i.e., number of standard deviations above zero) in the omit electron-density map*

Atom	*B*	Level	Atom	*B*	Level
P	30	15	C2	29	6
O1P	36	7	C1	34	9
O2P	32	7	O(−C1)	36	6
O3P	27	7	N	36	7
C4	27	4	O(−N)	36	6
C3	26	2.5			

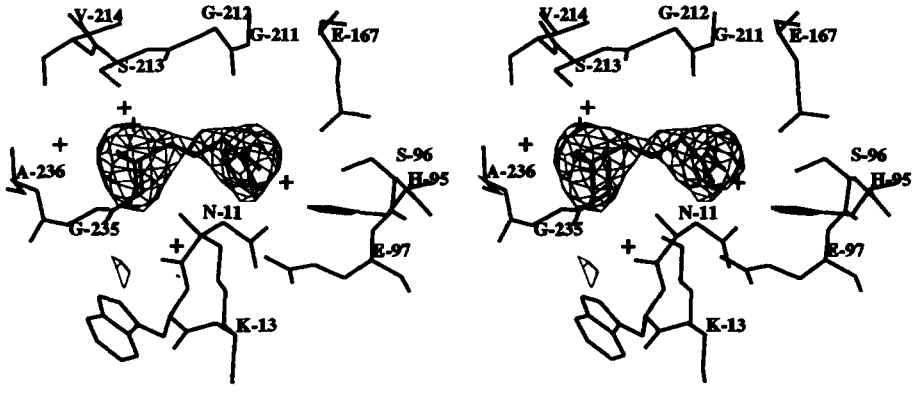

Fig. 2. Stereoscopic view of the fit of 4PBH into omit density at the active site of subunit 1. A model from which 4PBH was deleted was used to calculate F_c and phases for the calculation of an $mF_o - DF_c$ SIGMAA-weighted map. Shown here is the fit of the final 4PBH model into the resulting electron density. The map is contoured at three times its standard deviation.

planar about C3-C2, and (−)-synclinal for C3-C2-C1-O, i.e., the ligand is in a strainless conformation.

All potential hydrogen bond interactions of 4PBH are summarized in Figure 3 and Kinemage 3. The phosphonate group is directly coordinated by the main-chain NH group of Gly 235 and the OG of Ser 213. All other hydrogen bonds between the phosphonate and the protein are water mediated. Compared with other phosphate/phosphonate inhibitor complexes, where the inhibitor binds in the closed flexible loop environment, only the hydrogen bond with Gly 235 and the water-mediated interaction with Lys 13 are retained. It is of considerable interest to establish whether this altered binding mode leads to a different anion positioning. Therefore, a superposition was carried out of subunit 1 of the 4PBH complex and subunit 2 of the monohydrogen phosphate TIM complex (Verlinde et al., 1991a), which yielded an rms (root mean square) difference on CA positions of 0.30 Å. However, the P positions of inorganic phosphate and 4PBH are 1.54 Å apart.

At the other end of 4PBH the hydroxamyl oxygens are in contact with three electrophiles: the ND2 of Asn 11, the NZ of Lys 13, and the protonated NE2 of the neutral His 95 imidazole (Fig. 3). In addition, a water molecule mediates an interaction between the carbonyl oxygen of the hydroxamyl and the OG of Ser 96. Whether the 3.6-Å distance between the hydroxamyl nitrogen and the main-chain carbonyl of Gly 211 is indicative of a hydrogen bond is debatable. 4PBH also makes nonpolar interactions. Each of its three methylene groups is in contact with the CD1 of Ile 172: the distances are 3.2, 3.7, and 3.4 Å from, respectively, C2, C3, and C4 (Kinemage 3). At the present resolution, 2.84 Å, it is not clear whether the 3.0 Å between C2 and the main-chain carbonyl of Gly 211 is a bad contact. It is worthwhile mentioning that the catalytic residue Glu 167 is still in its "swung-out" conformation, i.e., χ_1 is (−)-synclinal, and is therefore unable to participate in the ligand binding.

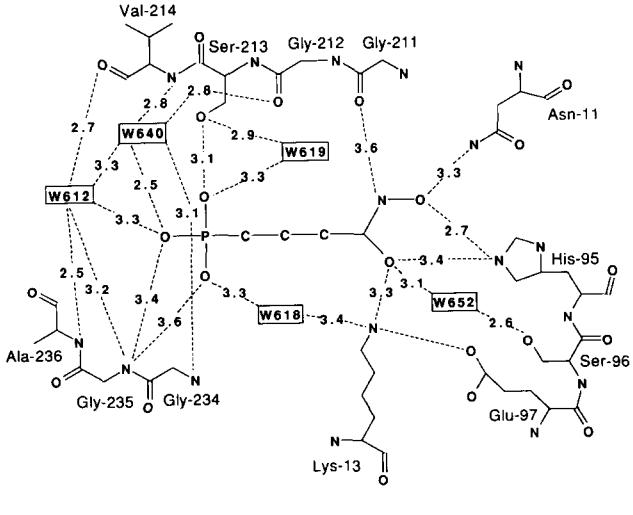

Fig. 3. Interactions between 4PBH and trypanosomal TIM. Potential hydrogen bonds are shown in dashed lines with the distances between donor and acceptor indicated in Ångstroms.

4PBH binding by subunit 2

The final difference Fourier map contoured at a 1.5σ level (Fig. 4) suggests the 4PBH binds also to the active site of subunit 2. Interestingly, the electron density also indicates that the side chain of Glu 467 adopts a "swung-in" conformation upon 4PBH binding, whereas there is no density for an alternative flexible loop conformation. In contrast to the binding of 4PBH to subunit 1, however, the ligand position is only partially occupied in the crystal. If the atomic signal of the putative P atom, which is 4σ, is compared with its counterpart in subunit 1 it leads to an estimated 0.25 occupancy. The low B-factors of the Glu 467 side chain (mean B value is 13.5 Å^2) in the "swung-out" conformation are also in accordance with a low occupancy for the alternative conformation. In view of the 2.84-Å resolution limit, no attempt was undertaken to build a 4PBH model into the density of subunit 2.

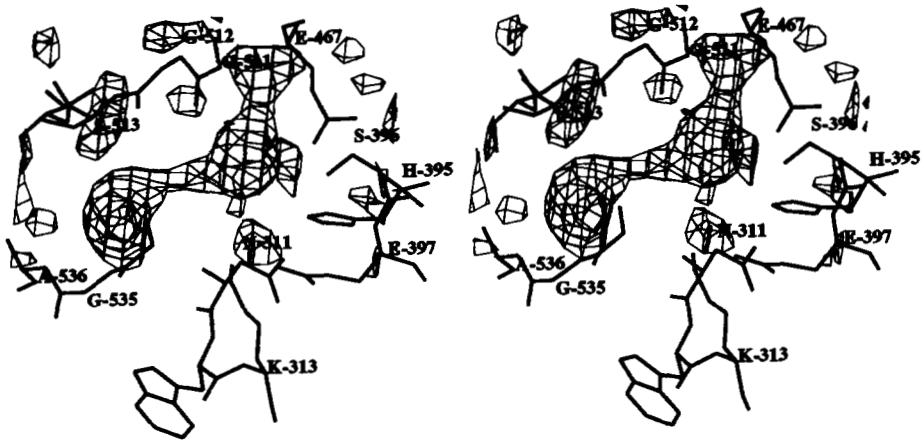

Fig. 4. Stereoscopic view of the electron density at the putative 4PBH binding site in subunit 2 of TIM, using the same map that was used for Figure 2. The map is contoured at 1.5 times its standard deviation, in contrast with the 3σ level of Figure 2.

Structural adaptation of TIM to ligand binding

It is possible to examine whether the presence of 4PBH alters the structure of the enzyme by comparing the crystal structure of the present trypanosomal TIM complex with the structure of the isomorphous unligated TIM crystals (Wierenga et al., 1991b). A least-squares superposition using the 498 CAs of the two structures yields an rms difference on CA atomic positions of 0.25 Å. On the basis of this superposition, not a single protein atom involved in the coordination of 4PBH at the active site of subunit 1, directly or water-mediated, reveals a difference in position of more than 0.61 Å. The presence of the ligand at that site has thus no detectable influence on the enzyme conformation. In contrast, at the active site of subunit 2 the low occupancy binding of 4PBH is accompanied by at least a change in the conformation of Glu 467.

Discussion

In the crystal phosphate or phosphonate-derived inhibitors like glycerol 3-phosphate, 3-phosphoglycerate, 3-phosphonopropionate (Noble et al., 1991b), and 2-phosphoglycerate (Noble et al., 1991a) bind to active site 2 of trypanosomal TIM with a concurrent closing of the flexible loop of the enzyme. This closure also occurs with inorganic phosphate (Verlinde et al., 1991a) or sulfate (Wierenga et al., 1991b). No binding has been observed with any of the aforementioned inhibitors in active site 1 of TIM where the flexible loop is fixed in an open conformation by crystal contacts. In contrast, the present study shows that 4PBH binds to both active sites of TIM, whereas in each case the flexible loop is in an open conformation. Full occupancy binding occurs in active site 1, and the occupancy is 25% in subunit 2. In addition, the position of the phosphor atom of 4PBH differs by 1.5 Å from that of phosphor seen in five other inhibitor complexes of *T. brucei* TIM with phosphates and phosphonates.

Related to the latter point is the question of why the flexible loop does not close down upon 4PBH binding in subunit 2 as was observed with the other phosphate/phosphonate inhibitors. Assuming that the full occupancy binding model of 4PBH in subunit 1 is also valid for subunit 2, a hint is possibly provided by the different phosphorus/sulfur position in the TIM complexes with inorganic phosphate, inorganic sulfate, and 4PBH. Inorganic phosphate is the deepest buried in the complex of the three ligands, whereas the flexible loop is in the completely closed conformation. Sulfate sits 0.9 Å further to the outside of the active site with the flexible loop in an almost closed conformation (Verlinde et al., 1991b); it still makes a hydrogen bond to NH of the flexible loop residue Gly 473. The P atom of 4PBH is yet another 0.6 Å further from the active site, thus making it very difficult to create a hydrogen bond between the phosphonate and Gly 473, if the flexible loop would be closed. The question remains why the phosphonate of 4PBH adopts this other position. Most likely, this is merely caused by the size of the inhibitor. 4PBH is conceptually one methylene unit longer than the substrate. Nevertheless, inside the active site it still interacts with the same residues (Asn 11, Lys 13, and His 95) responsible for binding the substrate and inhibitors like glycerol 3-phosphate without causing a conformational change of these residues. The extra spacer thus pushes the phosphonate further out of the active site and is allowed to do this because of the alternative anion-binding mode possibility.

An intriguing question concerning the present crystal form is why 4PBH binding to subunit 1 is preferred over binding to subunit 2. This is the more difficult to understand because the previous studies have shown that subunit 2 can be open (without inhibitor), almost closed (with sulfate), as well as fully closed (with phosphates or phosphonates). Therefore, the two binding sites were compared in detail. A least-squares superposition using CAs of subunit 1 and subunit 2 was carried out yielding an rms difference on CA atomic positions of 0.40 Å. After

omitting the OG of Ser 213/513, for which the electron density is heterogeneous in subunit 2, the rms difference for the 11 atoms directly involved in the binding of 4PBH was found to be 0.53 Å. Whether such small differences in atomic coordination can explain the differential binding in unclear. It remains puzzling, however, that poorer inhibitors such as phosphate (K_i = 5 mM [Verlinde et al., 1991a]), bind with full occupancy to subunit 2, whereas 4PBH, with a K_i of 0.33 mM, has an occupancy of only 25%. We have as yet no explanation for this observation.

It is instructive to compare the binding mode of 4PBH to *T. brucei* TIM with the binding of phosphoglycolohydroxamate (PGH) to yeast TIM (Davenport et al., 1991). PGH is a true transition-state analogue, having one methylene unit less than 4PBH and the phosphonate replaced by phosphate. It exhibits a K_i of 4 μM (Collins, 1974), which corresponds only to an 82-fold increase in binding affinity in comparison with 4PBH. Yet the interactions of the two inhibitors with TIM are very different and can be summarized as follows: (1) PGH binds in a closed flexible loop environment, whereas the loop is in an open conformation about 4PBH. Thus, PGH occupies with its phosphate function the "classical" phosphate-binding site, whereas 4PBH binds some 1.5 Å further to the outside of the active site. (2) The hydroxamyl-protein interactions with Lys 13 and His 95 appear to be similar for both inhibitors. However, in the yeast TIM-PGH complex the catalytic residue Glu 165 is in a "swung-in" conformation (χ_1 is (+)-synclinal) and has abstracted a proton from the hydroxamic function. As we do not observe a hydrogen bond between the N of 4PBH and Glu 167, which is in a "swung-out" conformation, it is likely that 4PBH binds to TIM as a dianion instead of a trianion because, according to Collins (1974), the pK_a of the hydroxamic acid is 9.5. (3) A further difference involves the nonpolar interactions. Extensive interactions are made between Ile 172 and the three methylene groups of 4PBH, whereas PGH interacts only with the CA of Gly 232. Consequently, it is not inconceivable that in the 4PBH-TIM complex, hydrophobic interactions compensate in part for a potentially poorer binding of the phosphonate and the hydroxamyl groups. (4) Internal strain of the inhibitors may also contribute to the difference in affinity, as discussed by Lolis and Petsko (1990) when they compared pairs of phosphate and phosphonate inhibitors. 4PBH is in a staggered conformation about the P-C4 bond. Hence, it does not have to pay the energetic price observed for the shorter phosphonate inhibitors like 3-phosphono-propionate, which are forced into an eclipsed conformation by the enzyme (Noble et al., 1991b). PGH, on the other hand, adopts an eclipsed conformation about the P-O bond: it is 42° away from the staggered conformation in one subunit and 32° in the second one (Davenport et al., 1991). In summary, the comparison of the two inhibitor complexes clearly shows that very similar inhibitors can have different binding modes. How this structural knowledge can be translated into relative binding affinities is not trivial and beyond the scope of this paper, also because desolvation of the inhibitors has to be considered.

For the further development of inhibitors of trypanosomal TIM, this study shows that it is possible to follow a new line of attack, namely to go for inhibitors that bind to the active site and at the same time prevent the closure of the flexible loop. The shift of the phosphonate with respect to its normal position and the open loop environment offer the possibility to branch 4PBH at C4 as can be seen in Table 2. In contrast to the inhibitors bound in a closed flexible loop environment, a large part of that carbon atom remains exposed in the complex with the enzyme. Work is currently underway to explore how such branching could lead to selective gTIM inhibitors.

Materials and methods

Purified trypanosomal TIM (Misset et al., 1986) was crystallized from 2.4 M ammonium sulfate in a 0.2 M MOPS (3-(*N*-morpholino)propanesulfonic acid) buffer, pH 7.0, containing also 1 mM EDTA, 1 mM dithiothreitol, and 1 mM sodium azide, as described previously (Wierenga et al., 1984). Because sulfate impairs ligand binding (the K_i of sulfate for trypanosomal TIM is 4.5 mM [Lambeir et al., 1987]), the crystals were transferred (Schreuder et al., 1988) to a 50% polyethyleneglycol 6000 solution containing 0.08 M ammonium sulfate and, subsequently, to a sulfate-free 50% polyethyleneglycol 6000 solution containing 3.3 mM 4PBH; all transfer solutions contained a 0.2 M MOPS buffer, pH 7.0, 0.6 mM EDTA, 0.6 mM dithiothreitol, and 0.6 mM sodium azide. Soaking took place for 65 days, with occasional transfer to fresh soaking solution during the first days. Data were collected on the Groningen FAST area detector system, using radiation from an Elliot GX21 rotating-anode generator. A single crystal with dimensions 0.25 × 0.2 × 0.1 mm^3 was used; the mosaic angle of the

Table 2. *Burial of molecular surface of 4PBH upon complex formation with gTIM: surface*[a] *of free and complexed 4PBH (Å^2)*

Atom	Free	Complex	Atom	Free	Complex
P	0.0	0.0	C2	18.3	0.0
O1P	20.4	14.4	C1	4.0	0.0
O2P	19.3	9.6	O(−C1)	19.0	8.8
O3P	25.2	18.1	N	13.0	0.0
C4	18.5	8.0	O(−N)	25.0	0.0
C3	13.4	2.2			

[a] Atomic van der Waals radii used in the calculations were P = 2.00 Å, O = 1.60 Å, C(H_2) = 1.90 Å, C(H) = 1.85, and N = 1.70 Å. Probe radius was 1.40 Å.

crystal was 0.7°. Data collection and initial data reduction were performed with the MADNES package (Messerschmidt & Pflugrath, 1987), with profile fitting being performed by the program XDS (Kabsch, 1988). Further merging and scaling was carried out with software of the Groningen BIOMOL crystallographic package. Statistics describing the data are shown in Table 3.

As we expected 4PBH to bind possibly with its phosphonate in an analogous position with respect to the previously determined phosphate/phosphonate inhibitor–TIM complexes, an initial $2mF_o - DF_c$ electron-density map, with coefficients as defined by Read (1986), was calculated using the presumed isomorphous crystal structure of a TIM complex with inorganic phosphate (Verlinde et al., 1991a), with all nonprotein atoms removed. Surprisingly, it was observed that although most regions of the protein fitted into the density of this map, no density was visible for the flexible loop of subunit 2 in its closed conformation. Instead, density for this loop was seen at the position it occupies in its open conformation; especially, the density of the voluminous Trp 470 makes it possible to distinguish between the two possible conformations of the flexible loop prior to crystallographic refinement. Consequently, the crystal structure of sulfate-free TIM (Wierenga et al., 1991a) (cell dimensions: a = 113.14 Å, b = 97.48 Å, c = 46.43 Å), where the flexible loop takes up the open conformation due to the absence of a ligand, was taken as a starting model for refinement. This sulfate-free structure had a conventional R-factor of 13.9% for data to 2.8 Å resolution, and good stereochemistry. Least-squares refinement of the TIM:4PBH complex was carried out using the TNT package (Tronrud et al., 1987). After initial refinement in which the individual monomers of TIM were treated as rigid bodies, 10 additional rounds of positional refinement and 10 rounds of strongly correlated B-factor refinement, with data between 6.0 and 2.84 Å, the R-factor dropped from 24.6 to 16.0%.

Table 3. *Data statistics for trypanosomal TIM complexed with 4PBH*

Parameter	Value
Space group	$P2_12_12_1$
Cell parameters	a = 113.34(8) Å, b = 97.15(4) Å, c = 46.45(6) Å
Maximum resolution	2.84 Å
Unique reflections	6,530
Completeness	95.8%
R_{merge}[a]	6.3% on intensities

[a] R_{merge} was calculated from the following equation:

$$[(\Sigma_h\Sigma_i|\bar{I}_h - I_{h,i}|)/\Sigma_h|\bar{I}_h|] \cdot 100\%.$$

At this point, a SIGMAA weighted difference Fourier map (Read, 1986) revealed density at a level of 9σ with a typical phosphate/phosphonate shape as the highest peak in the map near Gly 235 of subunit 1. Moreover, extra density at a level of 3σ was present near the catalytically important Lys 13, His 95, and Glu 167 of this subunit. Consequently, a 4PBH molecule was built into this density, taking the conformational preferences of hydroxamic acids as observed in the Cambridge Crystallographic Database (Allen et al., 1979) into account: (1) hydroxamic acids are cis-planar, and (2) the CH_2–CH_2–C=O dihedral of an attached aliphatic chain is (±)-synclinal. Also, a $2mF_o - DF_c$ map (Read, 1986) was used to rebuild some of the surface residue side chains. Eventually, the model for the side chain of Gln 319 was limited to CB and CG and for Glu 323 to CB due to the absence of interpretable density. It is worthwhile reiterating that Glu 323 is the residue thought to be responsible for preventing the binding of oxyanions in subunit 1 (Wierenga et al., 1991a). This residue, for which the B-factors of the carboxylate in the native structure are about 60 Å^2, is apparently even more disordered in the present structure. Further TNT refinement during which 53 water molecules were added smoothly converged to an R-factor of 11.5% (for statistics, see Table 4).

Molecular surface calculations were carried out using the program MS (Connolly, 1983) for the gTIM–4PBH complex and its individual constituents. Extended atomic radii were taken from McCammon et al. (1979) for protein atoms and derived by analogy for 4PBH.

Table 4. *Refinement statistics*

Parameter	Value
R-factor[a]	11.5%
Estimated coordinate error[b]	0.16 Å
Resolution range	6.0–2.84 Å
Reflections	6,530
Model	
Protein atoms	3,771
Water atoms	53
Ligand atoms	11
Root mean square deviations from ideal[c]	
Covalent bond lengths	0.01 Å
Bond angles	3.2°
B values	3.5 Å^2

[a] R-factor was calculated from the following equation:

$$[(\Sigma_h|F_{obs,h} - F_{calc,h}|)/\Sigma_h|F_{obs,h}|] \cdot 100\%.$$

[b] Estimated coordinate error was determined from a σ_A plot (Read, 1986).

[c] Root mean square deviations were calculated by TNT (Tronrud et al., 1987); for B-values, all covalently bonded atom pairs were included in the calculation.

Acknowledgments

We enjoyed stimulating discussions with Drs. Rik Wierenga and Martin Noble of the EMBL in Heidelberg. This research was supported by a grant of the WHO/UNDP/World Bank Special Programme for Research and Training in Tropical Diseases, by a fellowship from Hoffmann-La Roche, Basel, to C.L.M.J.V., and by the Netherlands Foundation for Chemical Research (S.O.N.) with financial aid from the Netherlands Organization for Scientific Research (N.W.O.). The coordinates of the TIM-4PBH complex have been submitted to the Brookhaven Protein Data Bank.

References

Allen, F.H., Bellard, S., Brice, M.D., Cartwright, B.A., Doubleday, A., Higgs, H., Hummelinck, T., Hummelinck-Peters, B.G., Kennard, O., Motherwell, W.D.S., Rogers, J.R., & Watson, D.G. (1979). The Cambridge crystal data centre: Computer-based search, retrieval, analysis, and display of information. *Acta Crystallogr. B35*, 2331-2339.

Collins, K.D. (1974). An activated intermediate analogue. The use of phosphoglycolohydroxamate as a stable analogue of a transiently occurring dihydroxyacetone phosphate-derived enolate in enzymatic catalysis. *J. Biol. Chem. 249*, 136-142.

Connolly, M.L. (1983). Analytical molecular surface calculations. *J. Appl. Crystallogr. 16*, 548-558.

Davenport, R.C., Bash, P.A., Seaton, B.A., Karplus, M.A., Petsko, G.A., & Ringe, D. (1991). Structure of the triosephosphate isomerase-phosphoglycolohydroxamate complex: An analogue of the intermediate on the reaction pathway. *Biochemistry 30*, 5821-5826.

Fairlamb, A.H., Opperdoes, F.R., & Borst, P. (1985). New approach to screening drugs for activity against African trypanosomes. *Nature 265*, 270-271.

Hol, W.G.J. (1986). Protein crystallography and computer graphics: Towards rational drug design. *Angew. Chem. Int. Ed. Engl. 25*, 767-778.

Kabsch, W. (1988). Evaluation of single-crystal X-ray diffraction data from a position-sensitive detector. *Acta Crystallogr. A21*, 916-924.

Knowles, J.R. (1991). Enzyme catalysis: Not different, just better. *Nature 350*, 121-124.

Lambeir, A.-M., Opperdoes, F.R., & Wierenga, R.K. (1987). Kinetic properties of triosephosphate isomerase from *Trypanosoma brucei brucei*. A comparison with the rabbit muscle and yeast enzymes. *Eur. J. Biochem. 168*, 69-74.

Lolis, E. & Petsko, G.A. (1990). Crystallographic analysis of the complex between triosephosphate isomerase and 2-phosphoglycolate at 2.5 Å resolution: Implication for catalysis. *Biochemistry 29*, 6619-6625.

Maquat, L.E., Chilcote, R., & Ryan, P.M. (1985). Human triosephosphate isomerase cDNA and protein structure. *J. Biol. Chem. 260*, 3748-3753.

McCammon, J.A., Woylnes, P.G., & Karplus, M. (1979). Picosecond dynamics of tyrosine side chains in proteins. *Biochemistry 18*, 927-942.

Messerschmidt, A. & Pflugrath, J.W. (1987). Crystal orientation and X-ray pattern prediction routines for area-detector diffractometer systems in macromolecular crystallography. *J. Appl. Crystallogr. 20*, 306-315.

Misset, O., Bos, O.J.M., & Opperdoes, F.R. (1986). Glycolytic enzymes of *Trypanosoma brucei*. Simultaneous purification, intraglycosomal concentrations and physical properties. *Eur. J. Biochem. 157*, 441-453.

Noble, M.E.M., Verlinde, C.L.M.J., Groendijk, H., Kalk, K.H., Wierenga, R.K., & Hol, W.G.J. (1991a). Crystallographic and molecular modelling studies on trypanosomal triosephosphate isomerase: A critical assessment of the predicted and observed structures of the complex with 2-phosphoglycerate. *J. Med. Chem. 34*, 2709-2718.

Noble, M.E.M., Wierenga, R.K., Lambeir, A.-M., Opperdoes, F.R., Thunnissen, A.-M.W.H., Kalk, K.H., Groendijk, H., & Hol, W.G.J. (1991b). The adaptability of the active site of trypanosomal triosephosphate isomerase as observed in the crystal structure of three different complexes. *Proteins Struct. Funct. Genet. 10*, 50-69.

Opperdoes, F.R., Wierenga, R.K., Noble, M.E.M., Hol, W.G.J., Wilson, M., Kuntz, D.A., Callens, M., & Perié, J. (1990). Unique properties of glycosomal enzymes. In *Parasites: Molecular Biology, Drug and Vaccine Design* (Cerami, T. & Agabian, N., Eds.), pp. 233-246. Wiley-Liss, New York.

Pompliano, D.L., Peyman, A., & Knowles, J.R. (1990). Stabilization of a reaction intermediate as a catalytic device: Definition of the functional role of the flexible loop of triosephosphate isomerase. *Biochemistry 29*, 3186-3194.

Read, R.J. (1986). Improved coefficients for maps using phases from partial structures with errors. *Acta Crystallogr. A42*, 140-149.

Schreuder, H.A., Groendijk, H., Van der Laan, J.M., & Wierenga, R.K. (1988). The transfer of protein crystals from their original mother liquor to a solution with a completely different precipitant. *J. Appl. Crystallogr. 21*, 426-429.

Swinkels, B.W., Gibson, W.C., Osinga, K.A., Kramer, R., Veeneman, G.H., van Boom, J.H., & Borst, P. (1986). Characterization of the gene for the microbody (glycosomal) triosephosphate isomerase of *Trypanosoma brucei*. *EMBO J. 5*, 1291-1298.

Tronrud, D.E., Ten Eyck, L.F., & Matthews, B.A. (1987). An efficient general-purpose least-squares refinement program for macromolecular structures. *Acta Crystallogr. A43*, 489-501.

Verlinde, C.L.M.J., Noble, M.E.M., Kalk, K.H., Groendijk, H., Wierenga, R.K., & Hol, W.G.J. (1991a). Anion binding at the active site of trypanosomal triosephosphate isomerase: Monohydrogen phosphate does not mimic sulphate. *Eur. J. Biochem. 198*, 53-57.

Verlinde, C.L.M.J., Rudenko, G., & Hol, W.G.J. (1991b). In search of new lead compounds for trypanosomiasis drug design: A protein structure-based linked-fragment approach. *J. Comput.-Aided Mol. Design 6*, 131-147.

Wierenga, R.K., Hol, W.G.J., Misset, O., & Opperdoes, F.R. (1984). Preliminary crystallographic studies of triosephosphate isomerase from *Trypanosoma brucei brucei*. *J. Mol. Biol. 178*, 487-490.

Wierenga, R.K., Noble, M.E.M., Postma, J.P.M., Groendijk, H., Kalk, K.H., Hol, W.G.J., & Opperdoes, F.R. (1991a). The crystal structure of the "open" and "closed" conformation of the flexible loop of trypanosomal triosephosphate isomerase. *Proteins Struct. Funct. Genet. 10*, 33-49.

Wierenga, R.K., Noble, M.E.M., Vriend, G., Nauche, S., & Hol, W.G.J. (1991b). Refined 1.83 Å structure of trypanosomal triosephosphate isomerase crystallized in the presence of 2.4 M ammonium sulphate. A comparison with the structure of the trypanosomal triosephosphate isomerase-glycerol-3-phosphate complex. *J. Mol. Biol. 220*, 995-1015.